Electronic Supporting Information

Novel cage-based metal−organic framework for efficient separation of light hydrocarbons

Muhammad Riaz[†,#], Dinesh Acharya[†,#], Hongxu Chu[†], Di Sun[†,*] Mohammad Azam[‡] and Ping Cui[†,*]

†School of Chemistry and Chemical Engineering, State Key Lab of Crystal Materials, Shandong University, Jinan 250100, P. R. China

‡Department of Chemistry, College of Science, King Saud University, PO BOX 2455 Riyadh, 11451 Saudi Arabia.

#These authors contribute equally.

Experimental Section

Reagents and General Procedures

All starting chemicals were purchased commercially and used without further purification. A Perkin-Elmer elemental analyzer was applied to collect Elemental data (C, H, and N). Room-temperature powder X-ray diffraction (PXRD) data were performed on a D/Max-2500 diffractometer and a Rigaku Oxford Diffraction XtaLAB Synergy-S diffractometer, using Cu Kα radiation (λ= 1.5418 Å). Simulation of the PXRD spectra was carried out by the single-crystal data and diffraction-crystal module of the Mercury (Hg) program available free of charge via the Internet at http://www.iucr.org. Thermogravimetric analyses (TGA) were performed with a TGA Q500 analyzer under a nitrogen flow to 800 °C. X-ray photoelectron spectroscopy (XPS) analysis was performed on a Kratos Axis Ultra DLD spectrometer with monochromatized Al Kα X-ray radiation as the X-ray source for excitation (hν = 1486.6 eV).

Synthesis of $\{[Co^{II}Co^{III}_2(\mu_3\text{-}O)](NDC)_3[Co^{II}TPyP(H_2O)]\cdot xS\}_n$ (S = solvent molecules): $CoSO_4\cdot 7H_2O$ (0.05 mmol, 0.0141g), H_2TPyP (0.0125 mmol, 0.0080 g), and H_2NDC (0.025 mmol, 0.0054g) were dissolved in a mixture solvent of CH_3CH_2OH (2.0 mL) and DMF (2.0 mL). The mixture was placed into a 25 mL Teflon-lined stainless-steel autoclave and kept in an oven at 120 °C. After 4 days, the reaction system was to cool to room temperature and red hexagonal-shaped crystals suitable for X-ray diffraction were obtained. The obtained microcrystals were washed with fresh DMF several times and collected by filtration in ~70% yield based on H_2Tpyp.

Formula is determined by considering the results of the single-crystal X-ray structure analysis, X-ray photoelectron spectroscopy (XPS), and previous reports.[1]

Single-Crystal X-ray Crystallography

Single-crystal X-ray diffraction measurement was carried out on a Rigaku Oxford Diffraction XtaLAB Synergy-S diffractometer using Cu Kα radiation (λ = 1.54184 Å) from PhotonJet micro-focus X-ray Source. An Oxford Cryosystems CryostreamPlus 800 cryostat was used to maintain the measuring temperature to be essentially constant at 100(2) K. Data were processed with the *CrysAlis*^{pro} software package.[2] The structure was solved successfully by intrinsic phasing methods implemented with ShelXT[3] and refined by full-matrix least-squares on F^2 ShelXL 2014[4] through the OLEX2 interface.[5] Anisotropic thermal parameters were assigned to all non-hydrogen atoms. Hydrogen atoms at carbon were geometrically calculated and refined as riding atoms. Appropriate restraints or constraints were used to the geometry and the atomic displacement parameters of the atoms in the cluster. Since, solvent molecules were heavily disordered, the SQUEEZE[6] method of PLATON was employed to remove scattering from disordered guest molecules residing in the pores. Additional crystallographic information has been summarized in Table S1. The contents of the solvent region are not represented in the unit cell contents in crystal data. Crystallographic data in CIF format has been deposited with the CCDC (No: 2368146).

Table S1. Crystal Data Collection and Structure Refinement for SDU-CP-**8**^{squeeze}.

Crystal number	SDU-CP-**8**^{squeeze}
Empirical formula	$C_{76}H_{42}Co_4N_8O_{14}$
Formula weight	1526.89
Temperature/K	99.99(11)
Crystal system	orthorhombic
Space group	*Immm*
a (Å)	18.8169(3)
b (Å)	19.4666(6)
c (Å)	37.5098(7)
α (°)	90
β (°)	90
γ (°)	90
V (Å^3)	13739.9(5)
Z	4
D_{calc} (g/cm^3)	0.738
μ (mm^{-1})	4.020
F(000)	3096.0
Radiation	Cu Kα (λ = 1.54184)
2*θ* range for data collection/°	6.534 to 132.526
Limiting indices	-22 ≤ h ≤ 17, -23 ≤ k ≤ 22, -43 ≤ l ≤ 24
Reflections collected / unique	18362 / 6248 [R(int) = 0.0307]
Completeness to theta = 25.027	95.6 %
Data/restraints/parameters	6248/503/303
Goodness-of-fit on F^2	1.104
$R_1{}^a$, $wR_2{}^b$ [$I > 2\sigma(I)$]	0.0796, 0.2393
R_1, wR_2 (all data)	0.0944, 0.2559
CCDC	2368146

Gas Sorption Measurements

Sample activation: As-synthesized crystals of SDU-CP-**8** (~80 mg) were washed several times with DMF and chloroform, respectively. And then, the sample was immersed in fresh chloroform for 5 days to exchange DMF solvent. Prior to gas measurement, this freshly prepared sample was activated by using the "outgas" function of the surface area analyser at 80 ℃ for 24 hours to obtain the fully evacuated frameworks. Finally, the sample was reweighed to determine the exact mass of the evacuated sample, and its properties were assessed using a volumetric method through analysis port of the gas adsorption instrument.

Isosteric Heat Calculation

The isosteric heat (Q_{st}) for the gas was analyzed with virial method previously reported in literatures.[7] The adsorption isotherms of CH_4, CO_2,C_2H_2, C_2H_4, C_2H_6, C_3H_6 and C_3H_8 at 273 and 298 K were fitted by Virial equation (1):

$$lnP = lnN + {}^{1}/_{T}\Sigma_{j=0}^{n} a_i N^i + \Sigma_{j=0}^{n} b_j N^j \qquad (1)$$

Herein, P (Pa) is the pressure, T (K) is the temperature, N (mg/g) is the amount adsorbed, m and n are the number of coefficients required to plot the isotherm, and a_i, b_j represent virial coefficients. Then, using the value of virial coefficient, the value of isothermal adsorption heat can be calculated by equation (2):

$$Q_{st} = -R\Sigma_{i=0}^{m} a_i N^i \qquad (2)$$

Prediction of gases adsorption selectivity by IAST

Based on the single-site Langmuir-Freundlich (L-F) model, isotherm data of the pure component for C_3H_8, C_2H_6, CH_4, C_2H_2, and CO_2 at 298 K was fitted. For SDU-CP-**8**, the adsorption selectivity of mixed C_3H_8/CH_4, C_2H_6/CH_4 and C_2H_2/CO_2 at 298 K was calculated using the ideal adsorbed solution theory (IAST) proposed by Myers and Prausnitz.[8] Single-site Langmuir-Freundlich (SSLF) model is listed as below:

$$q = \frac{a \times b \times p^c}{1 + b \times p^c} \qquad (3)$$

Where q (unit: mmol/g) is adsorbed amounts, p (unit: kPa) is the pressure of the bulk gas at equilibrium with the adsorbed phase, a (unit: mmol/g) is the saturation capacity, b (unit: 1/kPa) is the affinity coefficient, and c represent the deviation from an ideal homogeneous surface. Based on the pure component isotherm fits, the adsorption selectivity in a mixture can be formally defined as

$$S_{ads} = \frac{q_A / q_B}{y_A / y_B} \quad (4)$$

Where q_i (unit: mmol/g) represents the molar loading, y_i is the partial pressure of i in the mixture, and y_B = 1- y_A.

Breakthrough Experiments

The column breakthrough experiments were achieved on a mixSorb S dynamic sorption analyzer. The stainless-steel column (φ = 4 mm) packed with sample was first purged using helium flow for 2 hours at 90 ℃ before the breakthrough test. At room temperature, a gas mixture of 85% CH_4, 10% C_2H_6, and 5% C_3H_8 was introduced into the column at a flow rate of 5 mL/min. Similarly, a gas mixture of 25% C_2H_2, 25% CO_2, and 50% He was also introduced into the column at a flow rate of 3 mL/min. The effluent gas stream from the column was monitored by a mass spectrometer (MS) until complete breakthrough was achieved. The recyclability of SDU-CP-**8** for the separation of $C_3H_8/C_2H_6/CH_4$ were conducted under the same conditions.

Theoretical calculations

The Vienna Ab initio Simulation (VASP)[9,10] Package was used to do all the DFT computations. The electron-ion interaction was handled using a projector-augmented wave (PAW) potential,[11] while the electron-correlation interaction was handled using a generalized gradient approximation (GGA) with the Perdew-Burke-Ernzerhof (PBE) functional.[12] While calculating the conventional Kohn-Shan potential energy and inter-atomic forces, the traditional PBE function is incapable of describing non-bonded van der Waals (*vdW*) interaction that is dominant in the metal organic framework binding, a correction term of DFT-D3(BJ) method proposed by Grimme was added.[13] A k-point sampling[14] of 1×1×1 were used for the structural relaxation and electronic structure calculations, with the plane wave cutoff energy of 400 eV. Optimization were continued until the force on all atoms was smaller than 0.03 eV/Å. The adsorption energy is calculated as;

$$E_{ads} = E_{total} - E_{mof} - E_{gas} \quad (5)$$

Where, E_{total} is the total energy of a gas molecules adsorbed at MOF, and E_{mof} and E_{gas} are the energies of the MOF and individual gas, respectively. With the definition, it is obvious that the larger the adsorption energy, the stronger the interaction between gas molecule and MOF.

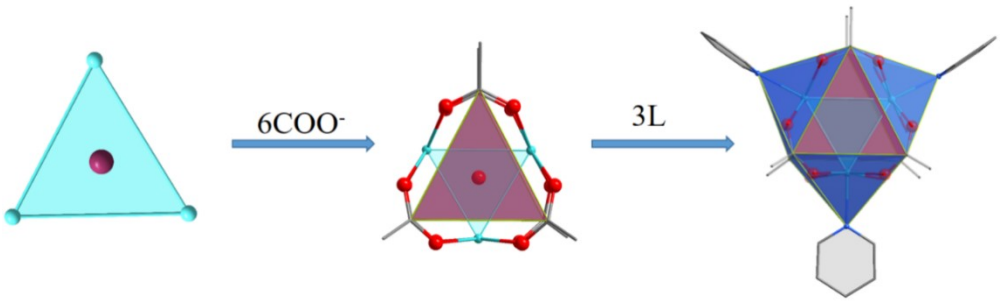

Figure S1. The cluster $[Co_3(\mu_3\text{-}O)(COO)_6L_3]$ (L = pyridyl group) of SDU-CP-**8**.

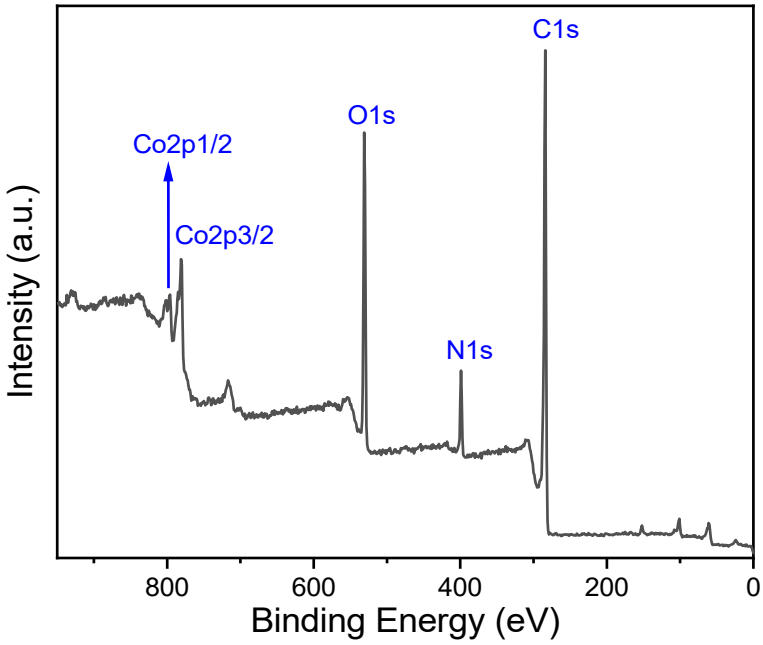

Figure S2. Survey XPS spectrum as-synthesized SDU-CP-**8**.

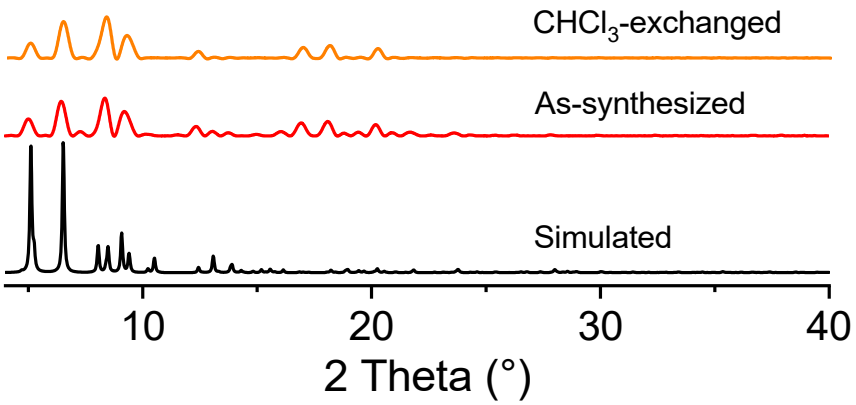

Figure S3. PXRD patterns for simulated (black), as-synthesized (red), and $CHCl_3$-exchanged (orange) forms of SDU-CP-**8**.

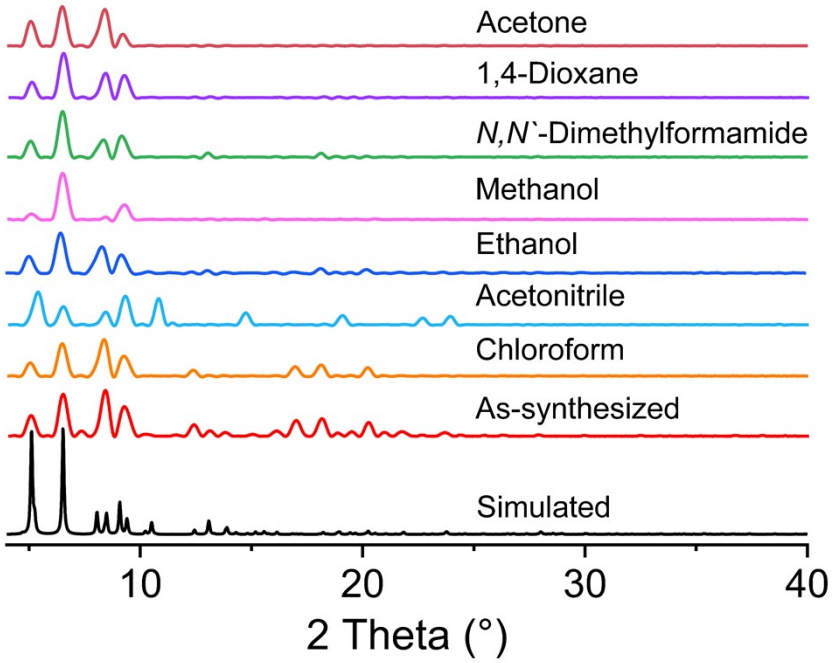

Figure S4. PXRD patterns of SDU-CP-**8** after being soaked in various organic solvents for 7 days.

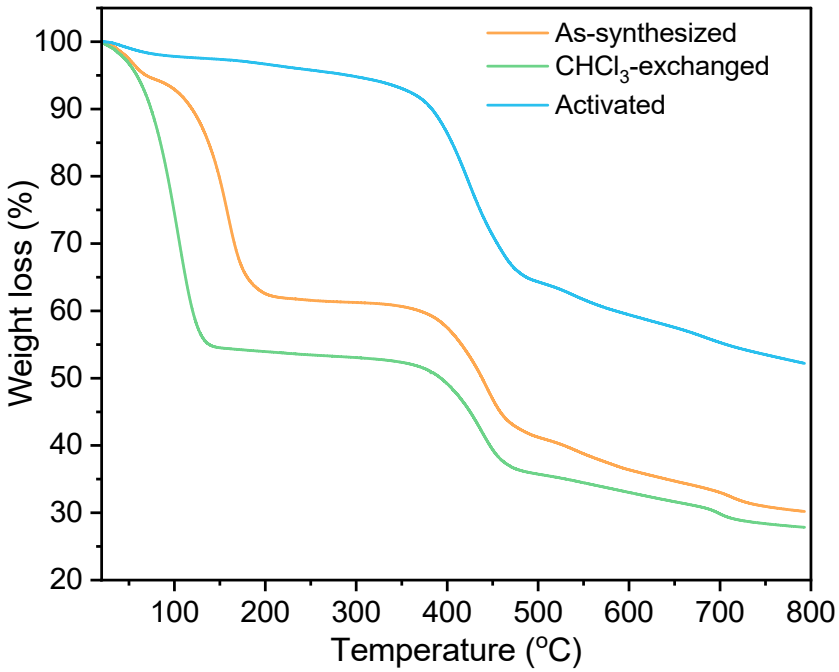

Figure S5. The TGA curves of SDU-CP-**8** for as-synthesized, $CHCl_3$-exchanged, and activated sample. The result showed that the framework of SDU-CP-**8** is stable up to 350 °C.

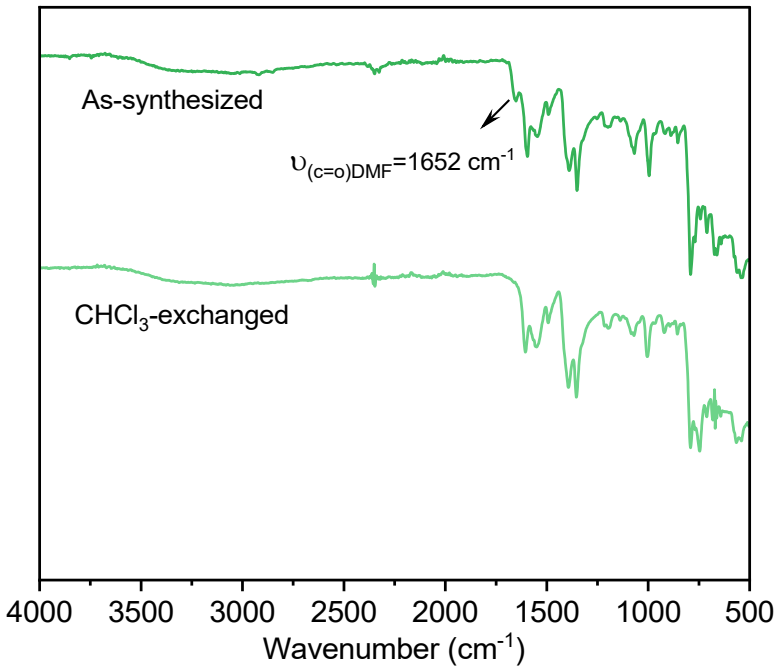

Figure S6. FT-IR spectrum of SDU-CP-**8** for as-synthesized and $CHCl_3$-exchanged sample.

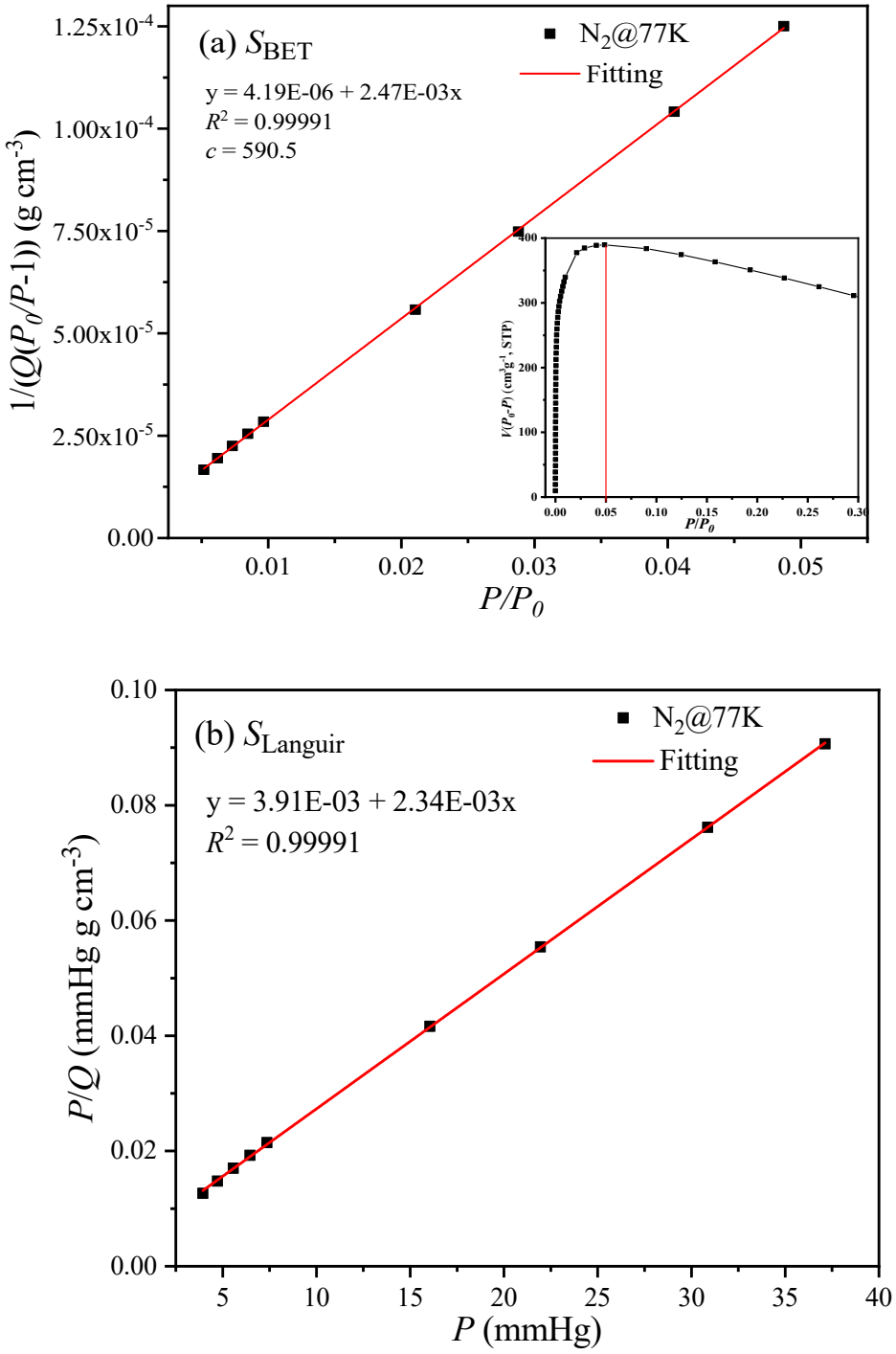

Figure S7. BET (a) and Langmuir (b) plots of SDU-CP-**8** obtained from N_2 adsorption isotherm at 77 K. Insert: plot of $Q(P_0\text{-}P)$ vs P/P_0, clearly showing that only the range below $P/P_0 \approx 0.05$ satisfies two major criteria established in literatures: (1) The pressure range selected should have values of $Q(P_0\text{-}P)$ increasing with P/P_0. (2) The y intercept of the linear must be positive to yield a meaningful value of the c parameter, which should be greater than zero.

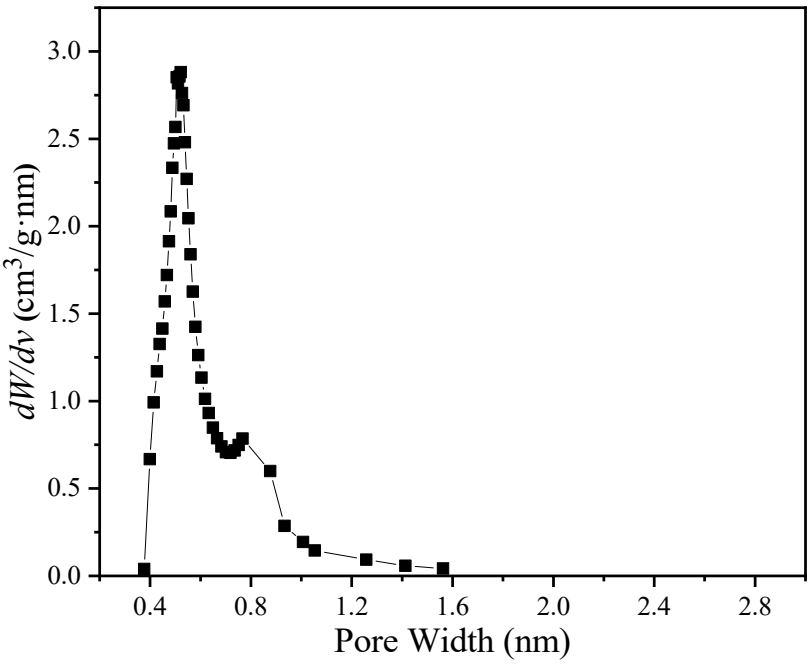

Figure S8. Pore size distribution of SDU-CP-**8** calculated by Horvath–Kawazoe mode.

Table S2: BET and Langmuir surface area comparison of some MOFs with tricapped trigonal prismatic SBUs

MOFs	BET(m^2/g)	Langmuir(m^2/g)	Ref.
SDU-CP-8	**1760**	**1860**	**This work**
FJU-90a	1572		15
SNNU-52	1180		16
SNNU-51	1170		16
MOF 2	1158		17
MOF 1	1124		17
Mn_3-BDC-TPT	938.8		18
Co-MOF1-tpt	826	1119	19
NbU-7-Cl	507.8	1050	20
Mn_3-BDC-TPP	282.3		18

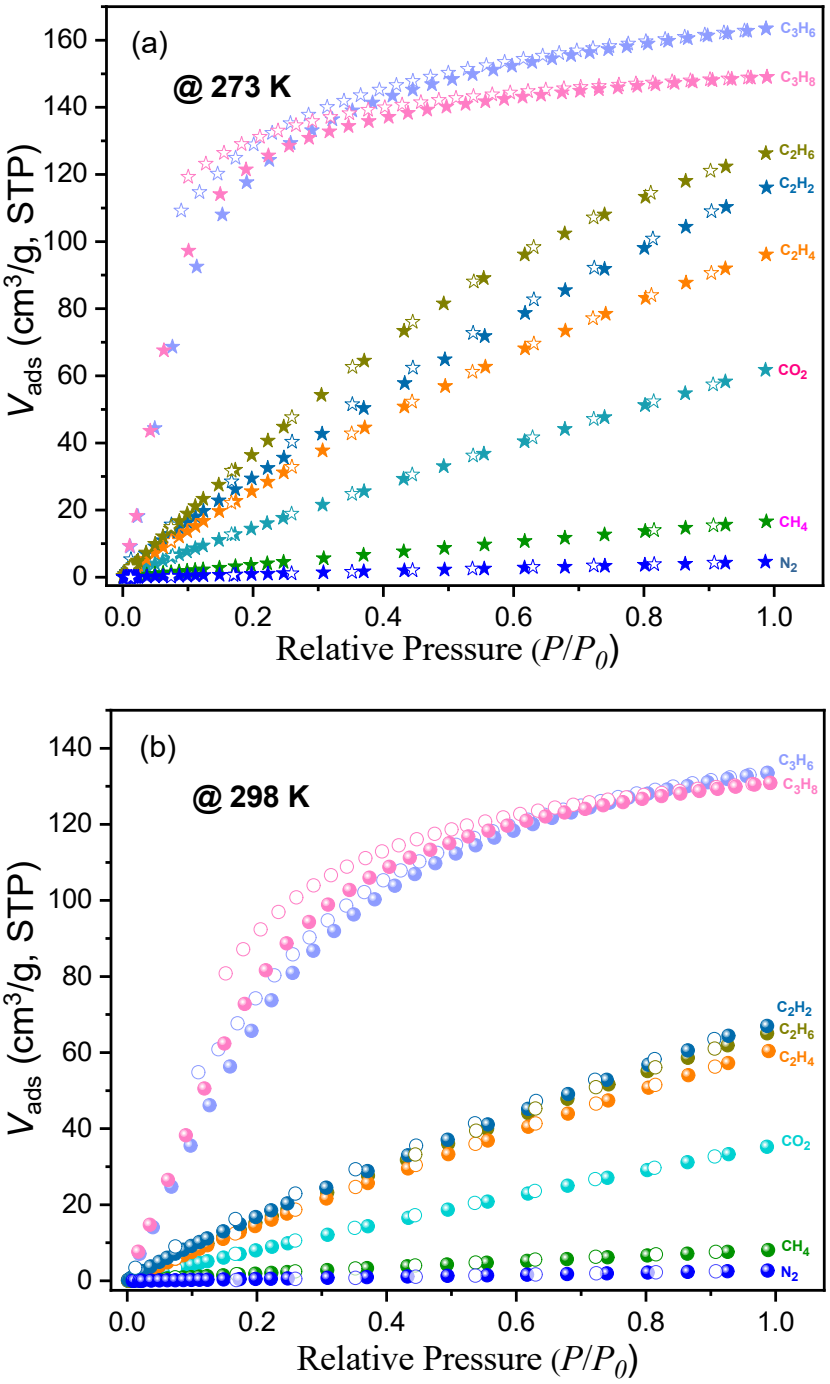

Figure S9. Sorption isotherms recorded on SDU-CP-**8** at 273 K (a) and 298 K (b). Adsorption and desorption branches are shown with solid and open symbols, respectively.

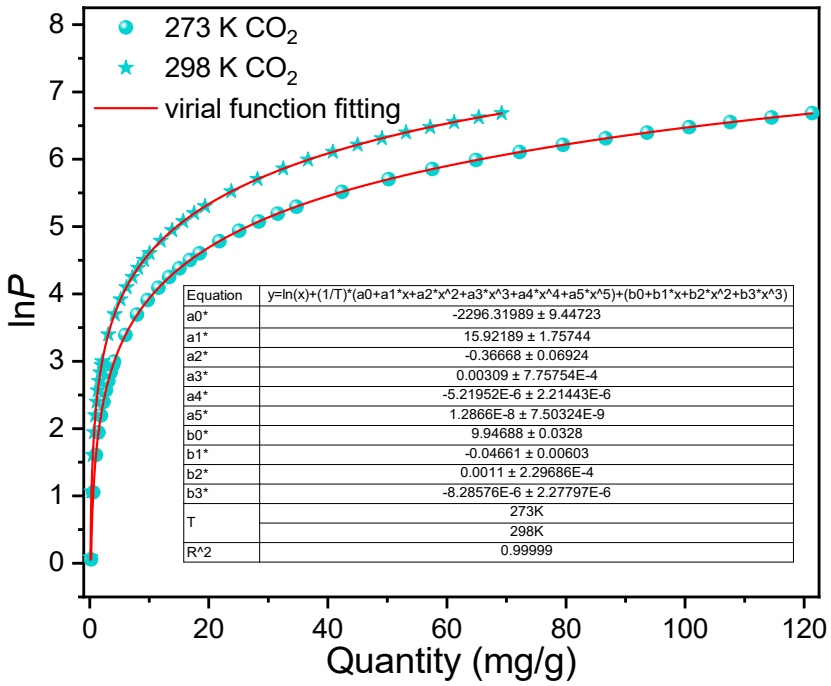

Equation	y=ln(x)+(1/T)*(a0+a1*x+a2*x^2+a3*x^3+a4*x^4+a5*x^5)+(b0+b1*x+b2*x^2+b3*x^3)
a0*	-2296.31989 ± 9.44723
a1*	15.92189 ± 1.75744
a2*	-0.36668 ± 0.06924
a3*	0.00309 ± 7.75754E-4
a4*	-5.21952E-6 ± 2.21443E-6
a5*	1.2866E-8 ± 7.50324E-9
b0*	9.94688 ± 0.0328
b1*	-0.04661 ± 0.00603
b2*	0.0011 ± 2.29686E-4
b3*	-8.28576E-6 ± 2.27797E-6
T	273K
	298K
R^2	0.99999

Figure S10. CO_2 adsorption isotherms of SDU-CP-**8** at 273 and 298 K (symbols) fitted by the virial equation (lines).

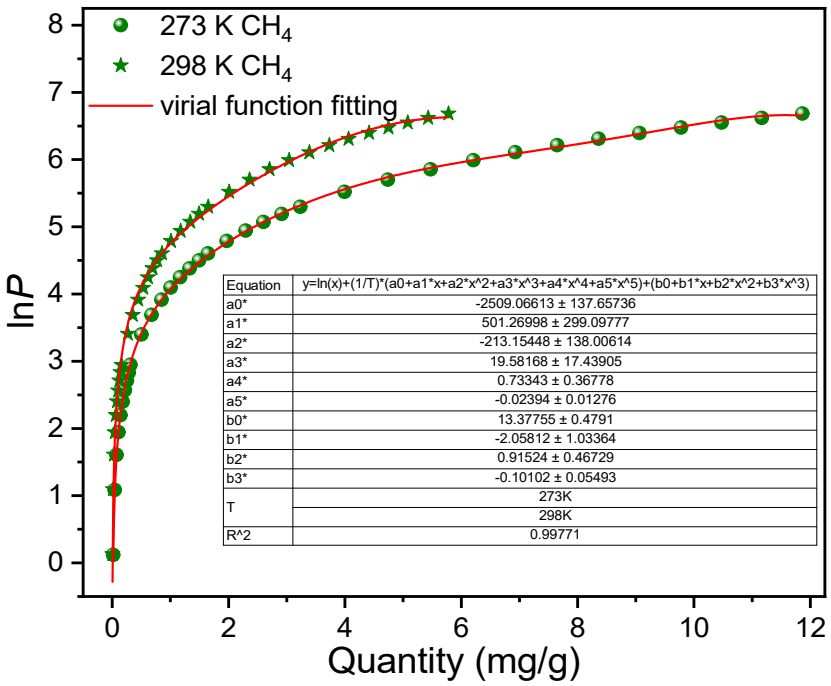

Equation	y=ln(x)+(1/T)*(a0+a1*x+a2*x^2+a3*x^3+a4*x^4+a5*x^5)+(b0+b1*x+b2*x^2+b3*x^3)
a0*	-2509.06613 ± 137.65736
a1*	501.26998 ± 299.09777
a2*	-213.15448 ± 138.00614
a3*	19.58168 ± 17.43905
a4*	0.73343 ± 0.36778
a5*	-0.02394 ± 0.01276
b0*	13.37755 ± 0.4791
b1*	-2.05812 ± 1.03364
b2*	0.91524 ± 0.46729
b3*	-0.10102 ± 0.05493
T	273K
	298K
R^2	0.99771

Figure S11. CH_4 adsorption isotherms of SDU-CP-**8** at 273 and 298 K (symbols) fitted by the virial equation (lines).

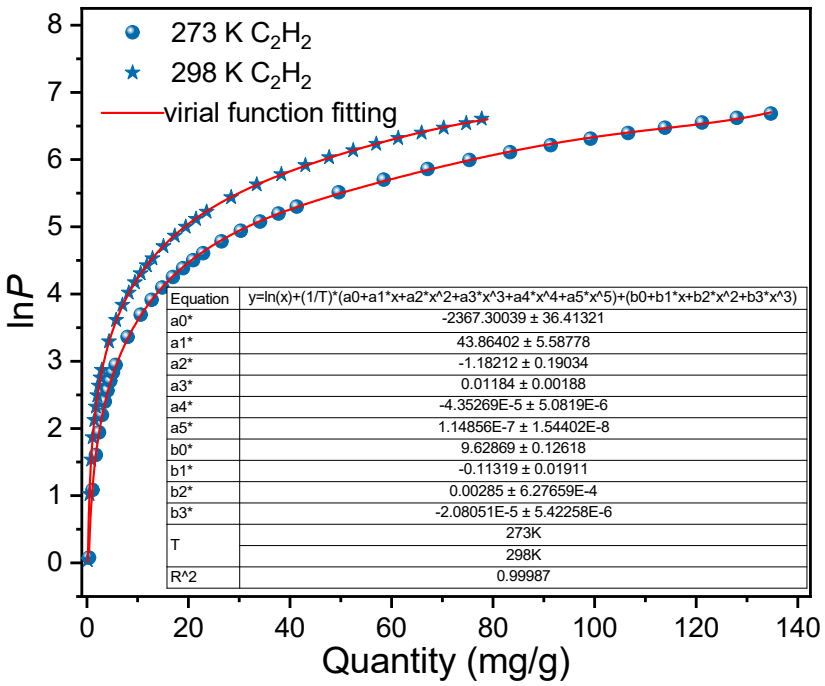

Equation	y=ln(x)+(1/T)*(a0+a1*x+a2*x^2+a3*x^3+a4*x^4+a5*x^5)+(b0+b1*x+b2*x^2+b3*x^3)
a0*	-2367.30039 ± 36.41321
a1*	43.86402 ± 5.58778
a2*	-1.18212 ± 0.19034
a3*	0.01184 ± 0.00188
a4*	-4.35269E-5 ± 5.0819E-6
a5*	1.14856E-7 ± 1.54402E-8
b0*	9.62869 ± 0.12618
b1*	-0.11319 ± 0.01911
b2*	0.00285 ± 6.27659E-4
b3*	-2.08051E-5 ± 5.42258E-6
T	273K
	298K
R^2	0.99987

Figure S12. C_2H_2 adsorption isotherms of SDU-CP-**8** at 273 and 298 K(symbols) fitted by the virial equation (lines).

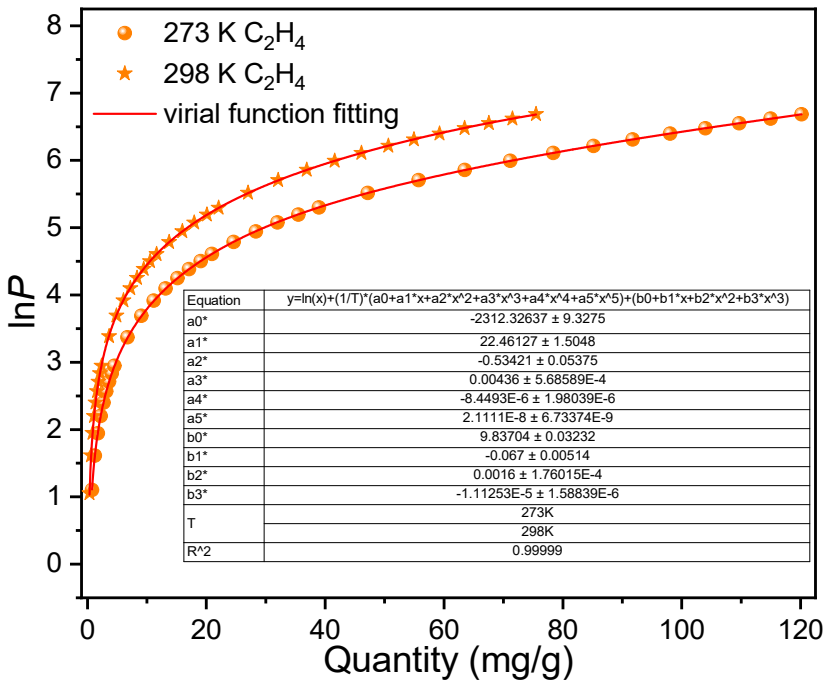

Equation	y=ln(x)+(1/T)*(a0+a1*x+a2*x^2+a3*x^3+a4*x^4+a5*x^5)+(b0+b1*x+b2*x^2+b3*x^3)
a0*	-2312.32637 ± 9.3275
a1*	22.46127 ± 1.5048
a2*	-0.53421 ± 0.05375
a3*	0.00436 ± 5.68589E-4
a4*	-8.4493E-6 ± 1.98039E-6
a5*	2.1111E-8 ± 6.73374E-9
b0*	9.83704 ± 0.03232
b1*	-0.067 ± 0.00514
b2*	0.0016 ± 1.76015E-4
b3*	-1.11253E-5 ± 1.58839E-6
T	273K
	298K
R^2	0.99999

Figure S13. C_2H_4 adsorption isotherms of SDU-CP-**8** at 273 and 298 K (symbols) fitted by the virial equation (lines).

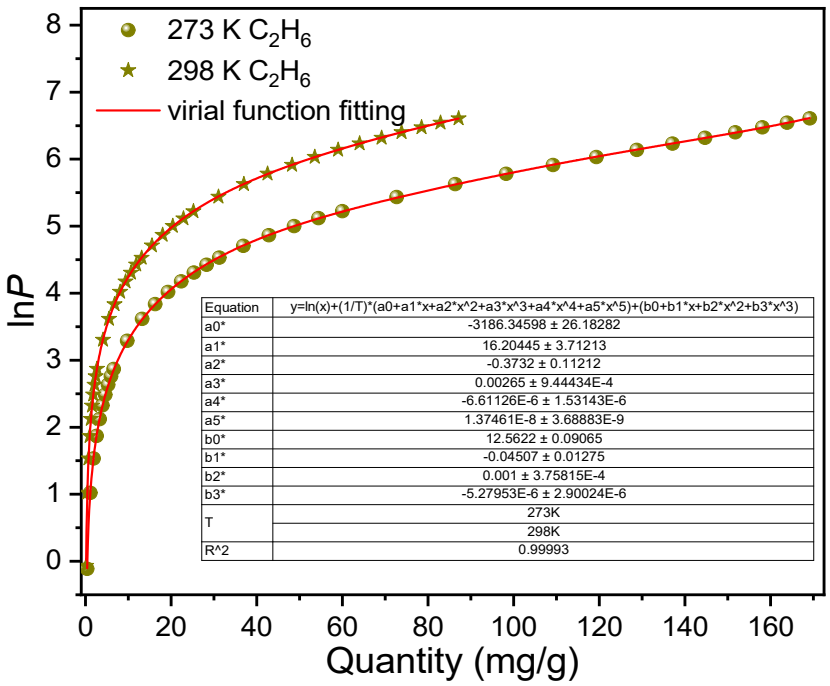

Equation	y=ln(x)+(1/T)*(a0+a1*x+a2*x^2+a3*x^3+a4*x^4+a5*x^5)+(b0+b1*x+b2*x^2+b3*x^3)
a0*	-3186.34598 ± 26.18282
a1*	16.20445 ± 3.71213
a2*	-0.3732 ± 0.11212
a3*	0.00265 ± 9.44434E-4
a4*	-6.61126E-6 ± 1.53143E-6
a5*	1.37461E-8 ± 3.68883E-9
b0*	12.5622 ± 0.09065
b1*	-0.04507 ± 0.01275
b2*	0.001 ± 3.75815E-4
b3*	-5.27953E-6 ± 2.90024E-6
T	273K
	298K
R^2	0.99993

Figure S14. C_2H_6 adsorption isotherms of SDU-CP-**8** at 273 and 298 K (symbols) fitted by the virial equation (lines).

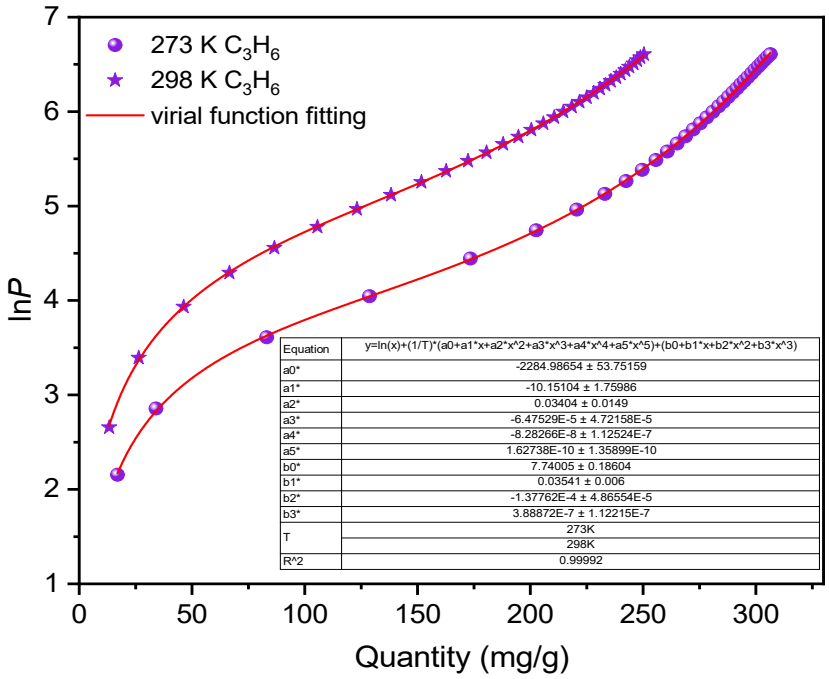

Figure S15. C_3H_6 adsorption isotherms of SDU-CP-**8** at 273 and 298 K (symbols) fitted by the virial equation (lines).

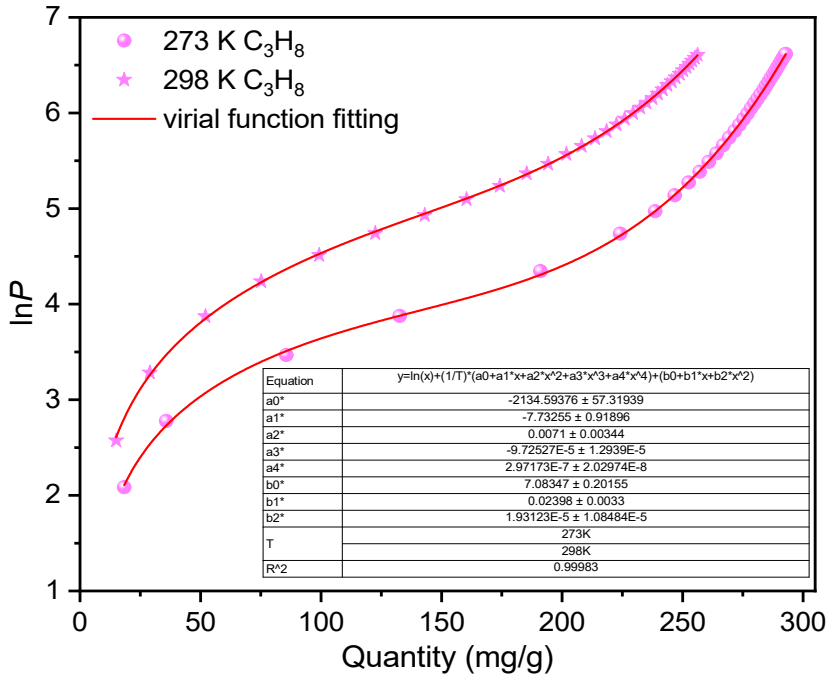

Figure S16. C_3H_8 adsorption isotherms of SDU-CP-**8** at 273 and 298 K (symbols) fitted by the virial equation (lines).

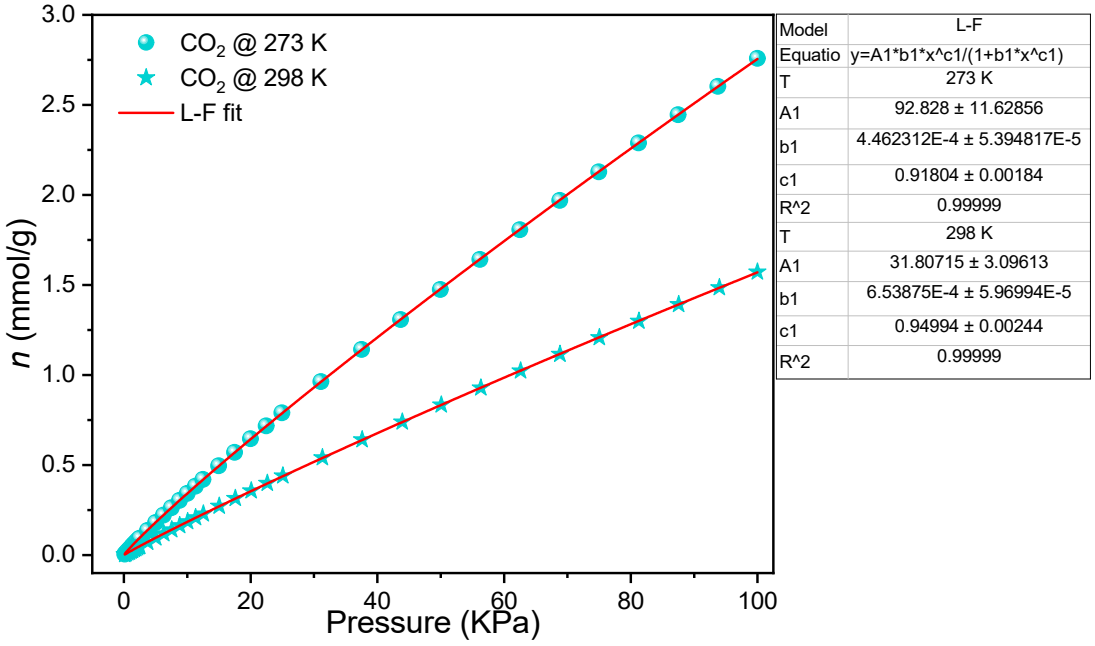

Model	L-F
Equatio	y=A1*b1*x^c1/(1+b1*x^c1)
T	273 K
A1	92.828 ± 11.62856
b1	4.462312E-4 ± 5.394817E-5
c1	0.91804 ± 0.00184
R^2	0.99999
T	298 K
A1	31.80715 ± 3.09613
b1	6.53875E-4 ± 5.96994E-5
c1	0.94994 ± 0.00244
R^2	0.99999

Figure S17. CO_2 adsorption isotherms of SDU-CP-**8** at 273 and 298 K (symbols) with fitting by L-F model (lines).

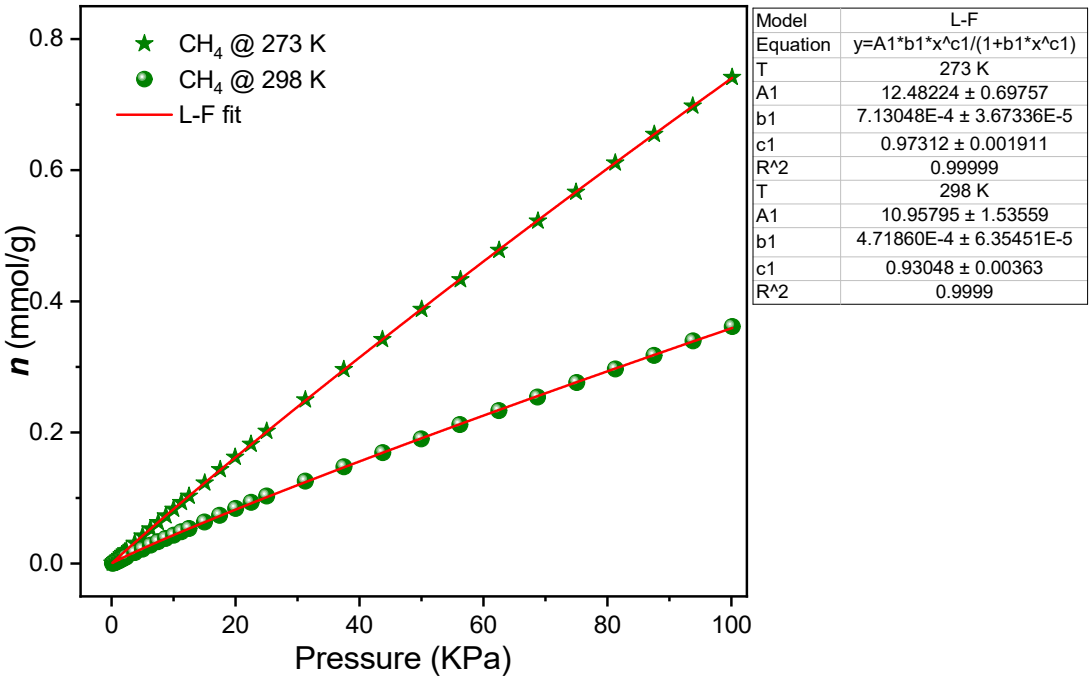

Model	L-F
Equation	y=A1*b1*x^c1/(1+b1*x^c1)
T	273 K
A1	12.48224 ± 0.69757
b1	7.13048E-4 ± 3.67336E-5
c1	0.97312 ± 0.001911
R^2	0.99999
T	298 K
A1	10.95795 ± 1.53559
b1	4.71860E-4 ± 6.35451E-5
c1	0.93048 ± 0.00363
R^2	0.9999

Figure S18. CH_4 adsorption isotherms of SDU-CP-**8** at 273 K and 298 K (symbols) with fitting by L-F model (lines).

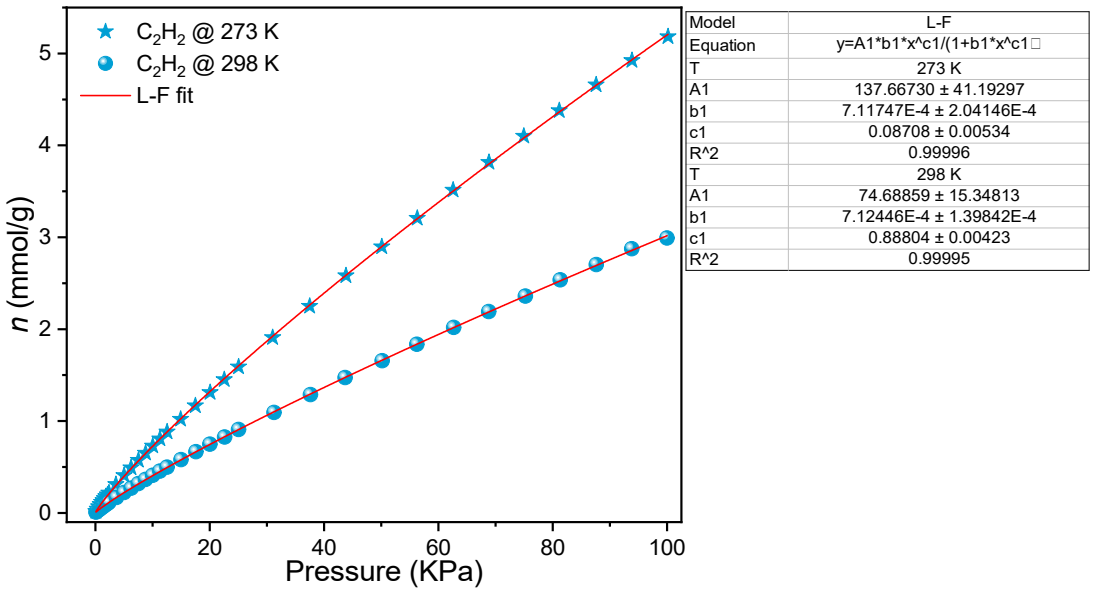

Model	L-F
Equation	y=A1*b1*x^c1/(1+b1*x^c1□
T	273 K
A1	137.66730 ± 41.19297
b1	7.11747E-4 ± 2.04146E-4
c1	0.08708 ± 0.00534
R^2	0.99996
T	298 K
A1	74.68859 ± 15.34813
b1	7.12446E-4 ± 1.39842E-4
c1	0.88804 ± 0.00423
R^2	0.99995

Figure S19. C_2H_2 adsorption isotherms of SDU-CP-**8** at 273 and 298 K (symbols) with fitting by L-F model (lines).

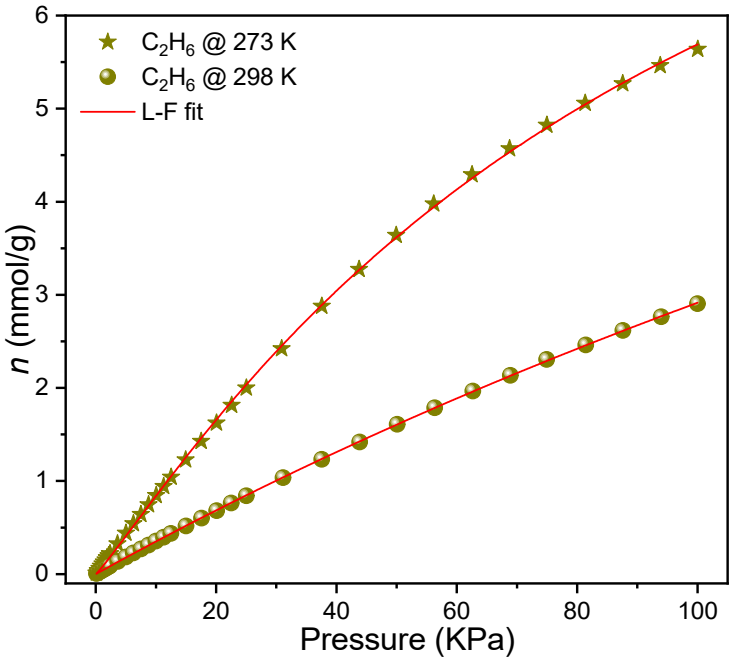

Model	L-F
Equation	y=A1*b1*x^c1/(1+b1*x^c1)
T	273 K
A1	11.41062 ± 0.35415
b1	0.00632 ± 1.30724E-4
c1	1.09864 ± 0.01415
R^2	0.99977
T	298 K
A1	16.09944 ± 0.77118
b1	0.00226 ± 8.059762E-5
c1	0.99777 ± 0.00521
R^2	0.99997

Figure S20. C_2H_6 adsorption isotherms of SDU-CP-**8** at 273 and 298 K (symbols) with fitting by L-F model (lines).

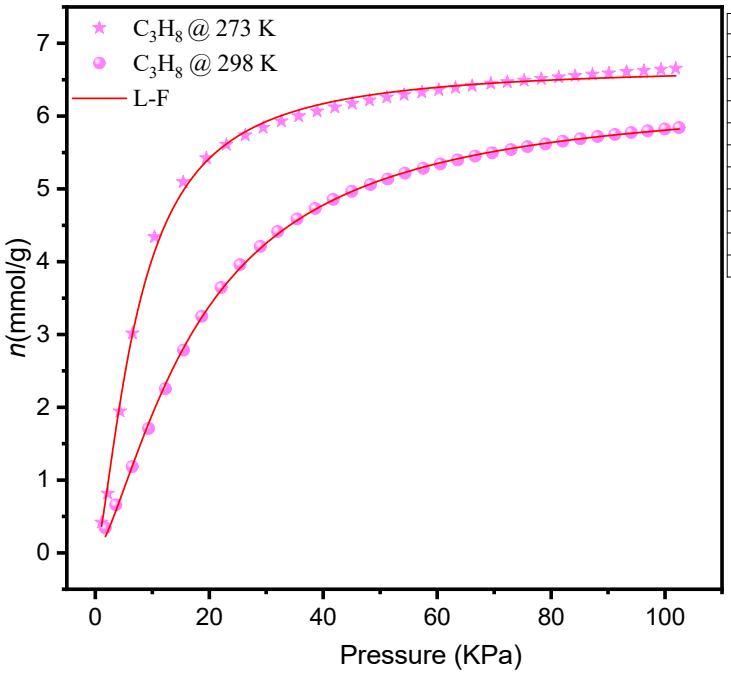

Model	L-F
Equation	y=A1*b1*x^c1/(1+b1*x^c1)
T	273 K
A1	6.69426 ± 0.03258
b1	0.00512 ± 0.00382
c1	1.47429 ± 0.00369
R^2	0.9979
T	298 K
A1	6.31047 ± 0.05007
b1	0.01616 ± 0.00129
c1	1.42647 ± 0.03138
R^2	0.9981

Figure S21. C_3H_8 adsorption isotherms of SDU-CP-**8** at 273 and 298 K (symbols) with fitting by L-F model (lines).

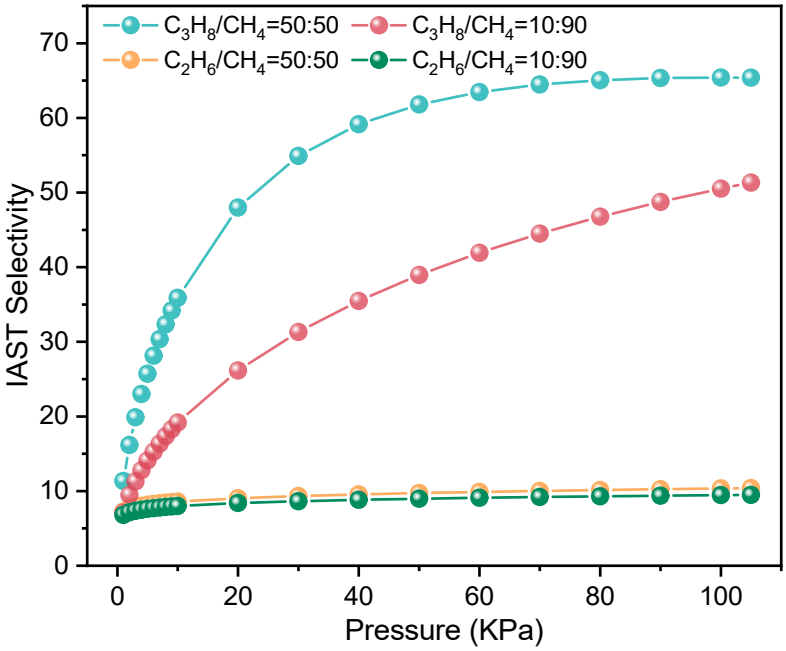

Figure S22. IAST selectivity of SDU-CP-**8** for C_3H_8/CH_4 (50:50, v/v) and C_2H_6/CH_4 (50:50, v/v) binary mixtures at different pressures.

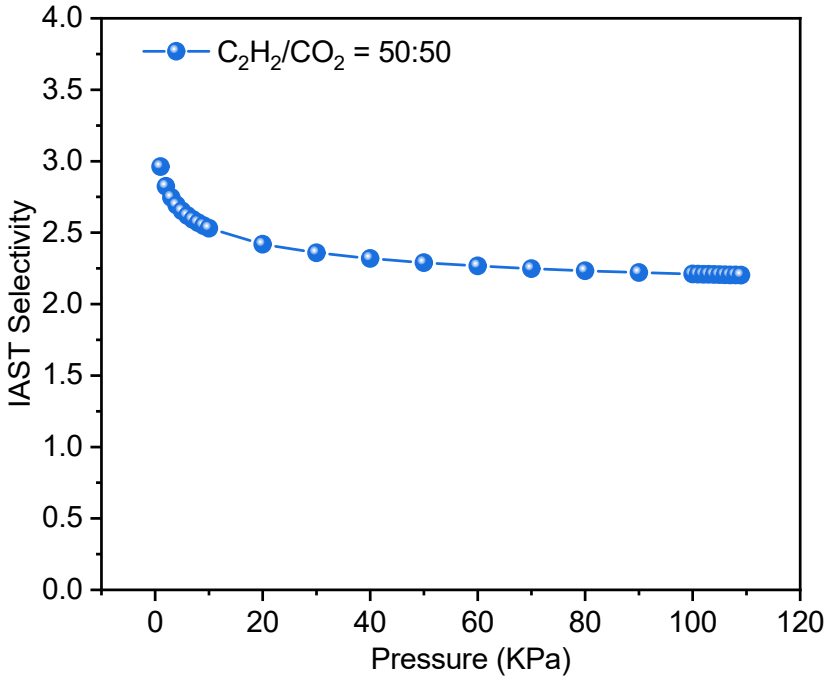

Figure S23. IAST selectivity of SDU-CP-**8** for C_2H_2/CO_2 (50:50, v/v) binary mixture at different pressures.

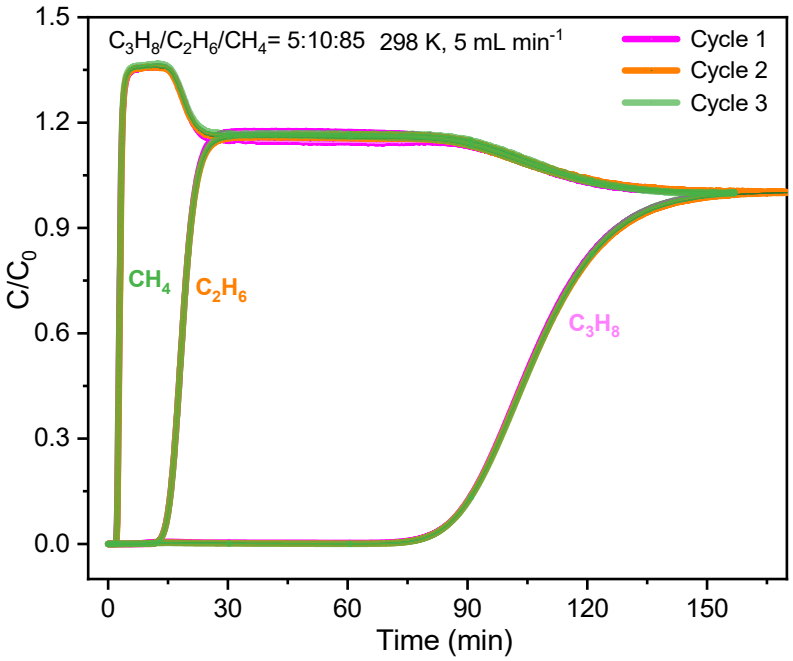

Figure S24. Repeated experimental breakthrough curves for gas mixture of $C_3H_8/C_2H_6/CH_4$.

References

(1) T. Zhang, Y. Q. Hu, T. Han, Y. Q. Zhai, Y. Z. Zheng, *ACS Appl. Mater. Interfaces* 2018, **10**, 15786−15792.

(2) Rigaku Oxford Diffraction. *CrysAlis^{Pro} Software system, version 1.171.40.25a*, Rigaku Corporation: Oxford, UK, 2018.

(3) G. M. Sheldrick, *Acta Cryst.* 2008, **A64**, 112−122.

(4) G. M. Sheldrick, *Acta Cryst.* 2015, **71**, 3−8.

(5) O. V. Dolomanov, L. J. Bourhis, R. J. Gildea, J. A. K. Howard, H. Puschmann, *J. Appl. Cryst*. 2009, **42**, 339–341.

(6) A. L. Spek, *Acta Cryst*. 2015, **71**, 9−18.

(7) B. Chen, X. Zhao, A. Putkham, K. Hong, E. B. Lobkovsky, E. J. Hurtado, A. J. Fletcher, K. M. Thomas, *J. Am. Chem. Soc*. 2008, **130**, 6411−6423; (b) J. L. C. Rowsell, O. M. Yaghi, *J. Am. Chem. Soc*. 2006, **128**, 1304–1315.

(8) A. L. Myers, J. M. Prausnitz, *AIChE J*. 1965, **11**, 121–127.

(9) G. Kresse and J. Furthmuller, *Comput. Mater. Sci*. 1996, **6**, 15−50.

(10) G. Kresse and J. Furthmuller, *Phys. Rev. B*, 1996, **54**, 11169−11186.

(11) G. Kresse and D. Joubert, *Phys. Rev. B,* 1999, **59**, 1758−1775.

(12) J. P. Perdew, K. Burke, M. Ernzerhof, *Phys. Rev. Lett.* 1996, **77**, 3865−3868.

(13) S. Grimme, *J. Comput. Chem*, 2006, **27**, 1787−1799.

(14) H. J. Monkhorst, J. D. Pack, *Phys. Rev, B.* 1976, **13**, 5188−5192.

(15) Y. Ye, Z. Ma, R. B. Lin, R. Krishna, W. Zhou, Q. Lin, Z. Zhang, S. Xiang, B. Chen, *J. Am. Chem. Soc*. 2019, **141**, 4130−4136.

(16) Y.-Y. Xue, S.-N. Li, Y.-C. Jiang, M.-C. Hu, Q.-G. Zhai, *J. Mater. Chem*. A, 2019, **7**, 4640−4650.

(17) D. M. Chen, J. Y. Tian, C. S. Liu, M. Chen, M. Du, *Chem. Eur. J.* 2016, **22**, 15035−15041.

(18) T. Zhang, J.-W. Cao, Y.-F. Dai, H. Feng, S.-Y. Zhang, J. Chen, T. Wang, Y. Wang, K.-J. Chen, *Cryst. Growth. Des.* 2022, **22**, 3594−3600.

(19) Q. Gao, X. L. Zhao, Z. Chang, J. Xu, X. H. Bu, *Dalton Trans.*, 2016, **45**, 6830−6833.

(20) J. Wu, Y. Wang, J. P. Xue, D. Wu, J. Li, *Inorg. Chem*. 2023, **62**, 19997−20004.